Acta Crystallographica Section B
Structural Science
ISSN 0108-7681

The compression mechanism of CrF_3

J.-E. Jørgensen,[a]* W. G. Marshall[b] and R. I. Smith[b]

[a]Department of Chemistry, University of Aarhus, DK-8000 Århus C, Denmark, and [b]ISIS Neutron Facility, Rutherford Appleton Laboratory, Chilton, Didcot, Oxon OX11 0QX, England

Correspondence e-mail: jenserik@chem.au.dk

Received 23 April 2004
Accepted 17 September 2004

The structure of CrF_3 has been studied in the pressure range from ambient to 9.12 GPa by time-of-flight neutron powder diffraction. Rietveld refinements of the crystal structure were performed in the space group $R\bar{3}c$ for all the recorded data sets. It was found that volume reduction is achieved through rotation of the CrF_6 octahedra and that the Cr—F—Cr bond angle decreases from 144.80 (7) to 133.9 (4)° within the investigated pressure range. Furthermore, a small octahedral strain was found to develop during compression. The octahedral strain reflects an elongation of the CrF_6 octahedra along the *c*-axis direction. The zero-pressure bulk modulus B_o and its pressure derivative B'_o were determined to be B_o = 29.2 (4) GPa and B'_o = 10.1 (3).

1. Introduction

Many metal trifluorides and trioxides with the formula MX_3, including CrF_3, crystallize in the rhombohedral VF_3-type structure for which the space group is $R\bar{3}c$. The structure of CrF_3 was first studied by X-ray diffraction by Jack & Maitland (1957) and later by Knox (1960). MX_3 compounds having the VF_3 structure are composed of corner-sharing MX_6 octahedra and they are therefore structurally related to the perovskite-type compounds AMX_3. A non-distorted perovskite-type compound is cubic with the space group $Pm\bar{3}m$, with the X atoms occupying a configuration of the cubic lattice complex J (*International Tables for Crystallography*, 1992, Vol. A), which corresponds to a sphere packing of the 8/3/*c*2 type with eight nearest-neighbour contacts per sphere (Fischer, 1973). The 8/3/*c*2 sphere packing of the X atoms constitutes a framework containing cubo-octahedral voids occupied by A atoms and octahedral voids occupied by M atoms. The ReO_3 structure is an example of a cubic perovskite-related compound with empty cuboctahedral voids (Meisel, 1932).

The VF_3 structure is derived from the ReO_3 structure by coupled rotations of the octahedra around one of the cubic body diagonals as $R\bar{3}c$ is a subgroup of $Pm\bar{3}m$. The empty cubo-octahedral voids permit relatively large tilts and rotations of the octahedra in the ReO_3 structure and the degree of space filling of a 8/3/*c*2 sphere packing can therefore be increased by rotating the octahedra around one of the body diagonals of the cubic unit cell. The octahedral voids are maintained during the rotation, while the empty cubo-octahedral voids will distort and diminish in volume. This type of deformation of the 8/3/*c*2 sphere packing suggests the simplest conceivable compression mechanism for an MX_3 compound with the space group $R\bar{3}c$. Rotation of the MX_6 octahedra around the *c*-axis direction will diminish the length of the *a* axis, and thereby the volume, while the length of the *c* axis is maintained during the rotation (assuming undistorted octa-

Table 1
Structural parameters for CrF_3 in a hexagonal setting.

P (GPa)	a (Å)	c (Å)	x	$100\langle u^2_{Cr}\rangle$ (Å^2)	$100\langle u^2_{F}\rangle$ (Å^2)	R_{wp}
0.0001	4.9863 (2)	13.2142 (7)	0.6153 (3)	0.32 (6)	0.63 (3)	0.0445
1.01	4.9106 (2)	13.2286 (9)	0.6271 (3)	0.08 (7)	0.63 (4)	0.0529
1.84	4.8593 (2)	13.2329 (9)	0.6338 (3)	0.21 (7)	0.63 (4)	0.0434
3.43	4.7860 (3)	13.237 (1)	0.6419 (6)	0.3 (1)	0.61 (5)	0.0604
5.43	4.7189 (2)	13.219 (1)	0.6514 (8)	0.18 (9)	0.63 (4)	0.0545
7.46	4.6639 (2)	13.192 (1)	0.658 (1)	0.17 (7)	0.58 (3)	0.0518
8.56	4.6382 (2)	13.172 (1)	0.660 (1)	0.10 (8)	0.44 (4)	0.0570
9.12	4.6265 (3)	13.163 (1)	0.659 (1)	0.1 (1)	0.21 (4)	0.0530

Space group: $R\bar{3}c$; Cr: 6(b) (0 0 0) and F: 18(e) (x 0 1/4).

hedra and a hexagonal setting of the space group). The compressibility in the a direction is expected to be high as the restoring force owing to the bending of the $M-X-M$ bonds. A 30° rotation around one of the body diagonals of the $Pm\bar{3}m$ structure leads to the hexagonal close packing of the framework atoms X and the $M-X-M$ bond angle decreases from 180° in the cubic $Pm\bar{3}m$ structure to 131.8° when hexagonal close packing of the X atoms is achieved. Close packing of the X atoms should give rise to an abrupt decrease in the compressibility. Further rotation of the octahedra leads to a 'super dense' sphere packing of the X atoms containing groups of three squeezed X atoms. Calcite $CaCO_3$ is an example of such a compound as carbon is located between three squeezed O atoms.

The non-distorted $Pm\bar{3}m$ structure is optimal for an MX_3 compound from an electrostatic point of view, as shown by Herzig & Zemann (1993). However, experimentally it is found that many metal tri-fluorides, MF_3, crystallize in the space group $R\bar{3}c$ with $M-F-M$ bond angles in the range 180–131.8°. ScF_3 is an example of a trifluoride close to the ReO_3 structure with an Sc—F—Sc bond angle of 175.8° and the space group was found to be *R32* (von Lösch *et al.*, 1982). RhF_3 represents the other extreme with hexagonally close-packed fluorine ions (Hepworth *et al.*, 1957). However, a small deviation from hexagonal close packing in RhF_3 was later observed by Grosse & Hoppe (1987). Bonding effects such as the polarizability of the fluorine ions as well as covalency were suggested to be responsible for the deviation from the non-distorted $Pm\bar{3}m$ structure (Herzig & Zemann, 1993).

The two VF_3-type compounds TiF_3 and FeF_3 have been studied by Sowa & Ahsbahs (1998), with both showing a pressure-induced octahedral strain and no structural transformations within the investigated pressure range. Furthermore, a recent high-pressure X-ray diffraction study of ReO_3 suggested that the compression of the $R\bar{3}c$ high pressure phase takes place through the rotation of the ReO_6 octahedra and that the O atoms become hexagonally close packed at 38 GPa, resulting in an abrupt decrease in the compressibility (Jørgensen *et al.*, 2000). However, no refinement of the crystal structure of the $R\bar{3}c$ phase was carried out in the studies of TiF_3, FeF_3 or the $R\bar{3}c$ phase of ReO_3. The aim of the present study was to obtain detailed structural information on the compression mechanism of CrF_3 for comparison with the isostructural compounds TiF_3 and FeF_3, as well as with the $R\bar{3}c$ high-pressure phase of ReO_3.

2. Experimental

The CrF_3 samples used in the present work were obtained from Aldrich Chemie (Aldrich catalogue number 44,976-8). High-pressure time-of-flight powder neutron diffraction patterns were recorded on the Polaris diffractometer at ISIS (Rutherford Appleton Laboratory, England) using the Paris–Edinburgh (P–E) pressure cell (Besson *et al.*, 1992). The sample was loaded into a TiZr encapsulated gasket (Marshall & Francis, 2002), along with a small amount of a fully deuterated 4:1 methanol:ethanol mixture to act as a pressure transmitting medium, and powder patterns were recorded in the pressure range from ambient to 9.12 GPa. The combined use of the methanol:ethanol mixture along with the encapsulated gasket ensures near-hydrostatic compression of the sample up to pressures of at least 9 GPa. Data were collected from two separate P–E cell loadings: one consisting of pure CrF_3 was used to determine its structural pressure dependence and the other a mixed-phase loading of CrF_3 and NaCl (a pressure standard) in the ratio 2:1 by volume, which was used to determine the room-temperature equation-of-state. Sample pressures for the mixed-phase loading were determined from the refined value for the NaCl lattice parameter by reference to the room-temperature equation-of-state for NaCl (Decker, 1971). Data analysis was performed by the Rietveld method using the *GSAS* suite of programs (Larson & Von Dreele, 1987).

3. Results and discussion

The recorded diffraction profiles of CrF_3 gave no indication of a structural phase transition within the investigated pressure range, so that all Rietveld refinements were performed in the space group $R\bar{3}c$. Small scattering contributions from WC and Ni originating from the anvils of the pressure cell were also included in the Rietveld refinements. Fig. 1 shows the observed, calculated and difference (obs − calc) powder neutron diffraction profiles of CrF_3 at 8.56 GPa, and the refined structural parameters at each of the measured pressures are given in Table 1.[1] For all pressures up to 8.56 GPa the parameters in Table 1 were refined using data collected from the pure CrF_3 loading, while those at the highest pressure, 9.12 GPa, were refined using a mixed-phase loading (CrF_3 plus an NaCl pressure standard) data set. The structural parameters for CrF_3 obtained at ambient pressure are in fair

[1] Supplementary data for this paper are available from the IUCr electronic archives (Reference: CK5004). Services for accessing these data are described at the back of the journal.

agreement with earlier results obtained by Jack & Maitland (1957) and Knox (1960).

Fig. 2 shows the a and c lattice parameters along with the relative volume V/V_o as a function of pressure. The a parameter decreases by 7.2% when the pressure is increased from ambient to 9.12 GPa, while c shows much less pressure dependence. As seen from Table 1, the c parameter increases by 0.17% to its maximum value at 3.43 GPa and then decreases smoothly above this pressure. The increase in c is associated with small distortions of the CrF_6 octahedra, as explained below. Larger increases in c during compression were also observed in the case of TiF_3 and FeF_3 (3.3 and 1.1%, respectively; Sowa & Ahsbahs, 1998). Overall the pressure dependence of the a- and c-lattice parameters for CrF_3, TiF_3 and FeF_3 show that volume reduction of these compounds takes place through the rotation of the octahedra around the c axis.

The unit-cell volumes derived from the mixed-phase loading data were used in the determination of the initial bulk modulus B_o and its pressure derivative B'_o for CrF_3 by use of the third-order Birch–Murnaghan equation-of-state

$$P = (3/2)B_o(x^{-7/3} - x^{-5/3})[1 - (3/4)(4 - B'_o)(x^{-2/3} - 1)], \quad (1)$$

where x denotes the volume ratio V/V_o with V_o being the volume at zero pressure, while B_o and B'_o are the isothermal bulk modulus at ambient pressure and its pressure derivative, respectively. The least-squares fit to the measured data yields the following value for the bulk modulus: B_o = 29.2 (4) GPa and B'_o = 10.1 (3). The low value of B_o is due to the fact that compression is achieved through bending of chemical bonds. Bond bending is also the reason for the large compressibility of the $Im\bar{3}$ phase of ReO_3, which has B_o = 35 (1) GPa. In comparison, compression of the cubic $Pm\bar{3}m$ phase takes place through compression of the Re—O bonds, yielding a much higher B_o value of 100 (18) GPa (Jørgensen *et al.*, 2000). The B'_o value obtained of 10.1 (3) is consistent with the fact that most materials have values ranging from 2 to 12, soft materials having large B'_o values in contrast to the typical value of $B'_o \simeq 4$.

Fig. 3 shows the CrF_3 structure at 9.12 GPa. Symmetry allows for two independent F—F distances within each CrF_6

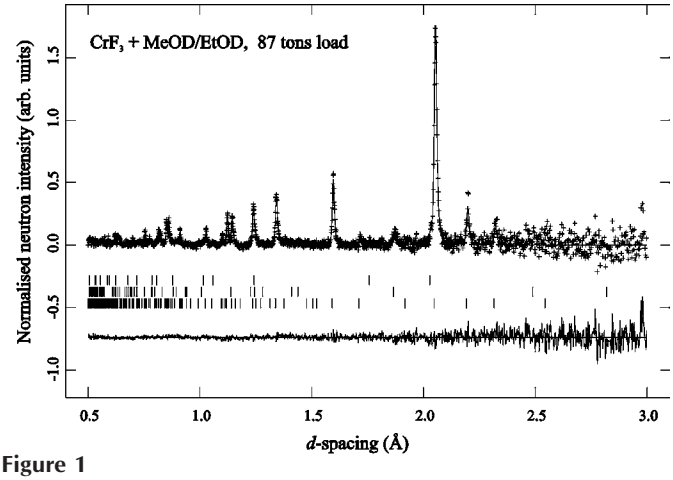

Figure 1
Powder neutron diffraction pattern obtained from CrF_3 at 8.56 GPa. The crosses and the solid line represent the measured and calculated patterns, respectively. The lower curve shows the difference between observed and calculated intensities. From the bottom to the top the vertical tick marks shown represent the Bragg reflection positions for CrF_3, WC and Ni, respectively. The weak contributions to the pattern from WC and Ni arise from the anvils of the pressure cell.

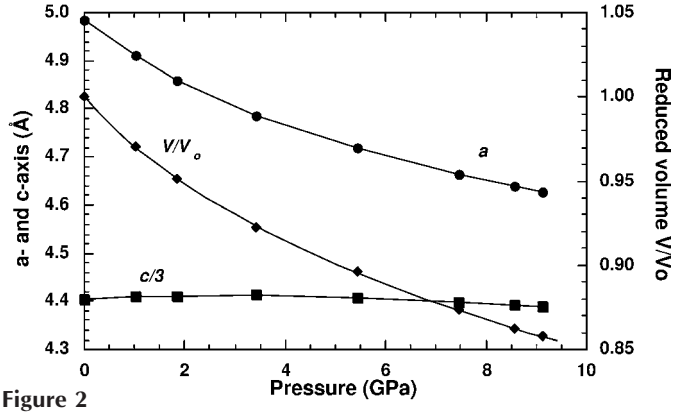

Figure 2
Lattice parameters a, c and the relative volume V/V_o plotted as a function of pressure. The solid curve for the relative volume represents a fit to the third-order Birch–Murnaghan equation-of-state with bulk modulus B_o = 29.2 (4) GPa and its pressure derivative B'_o = 10.1 (3), as described in the text. The estimated standard deviations on a, c and V/V_o are smaller than the plotted symbols and the solid curves for the lattice parameters a, c are guides to the eye.

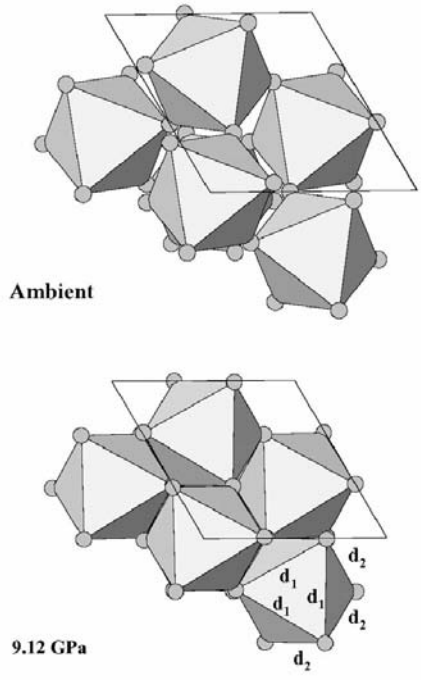

Figure 3
The CrF_3 structure at ambient pressure and 9.12 GPa viewed along the c axis. Symmetry allows for two independent F—F distances d_1 and d_2 within each CrF_6 octahedron, as marked on the lower figure. The octahedral strain is due to an elongation of the octahedra along the c axis with d_1 = 2.641 (5) Å and d_2 = 2.672 (2) Å at 9.12 GPa. The hexagonal unit cell is shown with solid lines.

octahedron. The short and long F—F distances, denoted here as d_1 and d_2, are found within and out of the basal plane, respectively. Figs. 4 and 5 show the structural changes of CrF_3 during compression. From Fig. 4(*a*) it is seen that the structural changes of the CrF_6 octahedra are minor during compression. The short and long F—F distances are reduced by 1.6 and 0.80%, respectively, while the Cr—F bond is shortened by 1.2%. Furthermore, d_1 exhibits a change in slope at 3.43 GPa, while d_2 decreases smoothly with increasing pressure. The octahedral strain ε defined as $\varepsilon = (d_2 - d_1)/(d_2 + d_1)$ is shown in Fig. 4(*b*). This quantity increases linearly to a value of 4.5×10^{-3} at 3.43 GPa and then stays roughly constant above this pressure. The difference in the pressure dependences of d_1 and d_2 below 3.43 GPa explains the increase in ε, which reflects an increasing rhombohedral distortion of the CrF_6 octahedra as they become elongated along the *c* direction. The increasing octahedral strain is consistent with the pressure dependence of the *c* lattice parameter described above. Analysis of the results of Sowa & Ahsbahs (1998) for TiF_3 and FeF_3 shows that ε also increases linearly up to *ca* 3 GPa and saturates at values of 1.4×10^{-2} and 6.3×10^{-3} for TiF_3 and FeF_3, respectively. No structure refinements were reported in the high-pressure diffraction study of TiF_3 and FeF_3, and the F—F distances d_1 and d_2 were calculated under the assumption that the metal—fluorine bond length is independent of the pressure. The ε values for these compounds should therefore be considered as lower limits for the octahedral strain, as they will increase if the metal—fluorine bond length is shortened. The pressure-induced octahedral strain was attributed to repulsive interactions between the cations in the case of FeF_3, TiF_3 and $NaSbF_6$ (Sowa & Ahsbahs, 1998; Sowa, 1997). The Cr—F—Cr bond angle, shown in Fig. 5, decreases from 144.80 (7) to 133.9 (4)°, showing that the F atoms are almost hexagonally close packed at 9.12 GPa, the highest pressure reached in this study. Furthermore, no systematic changes of the F—Cr—F angles within the CrF_6 octahedra were observed as a function of pressure. This again shows that volume reduction is achieved primarily through rotation of the CrF_6 octahedra around the *c*-axis direction.

The rotation angle φ of the CrF_6 octahedra around the *c* direction may be calculated from the fluorine *x* coordinates given in Table 1 and is shown as a function of pressure in Fig. 5. A coordinate value of $x = 1/2$ corresponds to the cubic $Pm\bar{3}m$ structure ($\varphi = 0°$), while the rhombohedral $R\bar{3}c$ structure with hexagonally close-packed F atoms within the basal plane is obtained for $x = 2/3$ ($\varphi = 30°$). From Table 1 it is seen that *x* saturates at a value of 0.660 (1) at *ca* 8 GPa (corresponding to $\varphi = 28.8°$). We therefore conclude that the F atoms become hexagonally close packed within the basal plane at this pressure. The $3^{1/2}c/3a$ ratio for a $R\bar{3}c$ structure with hexagonally close-packed F atoms corresponds to the conventional *c*/*a* ratio for a hexagonal sphere packing. From the data in Table 1 it is found that the average value of the $3^{1/2}c/3a$ ratio is 1.6411 at pressures above 8 GPa, which is close to the ideal *c*/*a* ratio value of 1.633 for a hexagonal close packing of spheres, thereby corroborating the suggestion of close-packed F atoms in CrF_3 at high pressure. The accessible pressure range was not large enough to observe an abrupt enhancement of the bulk

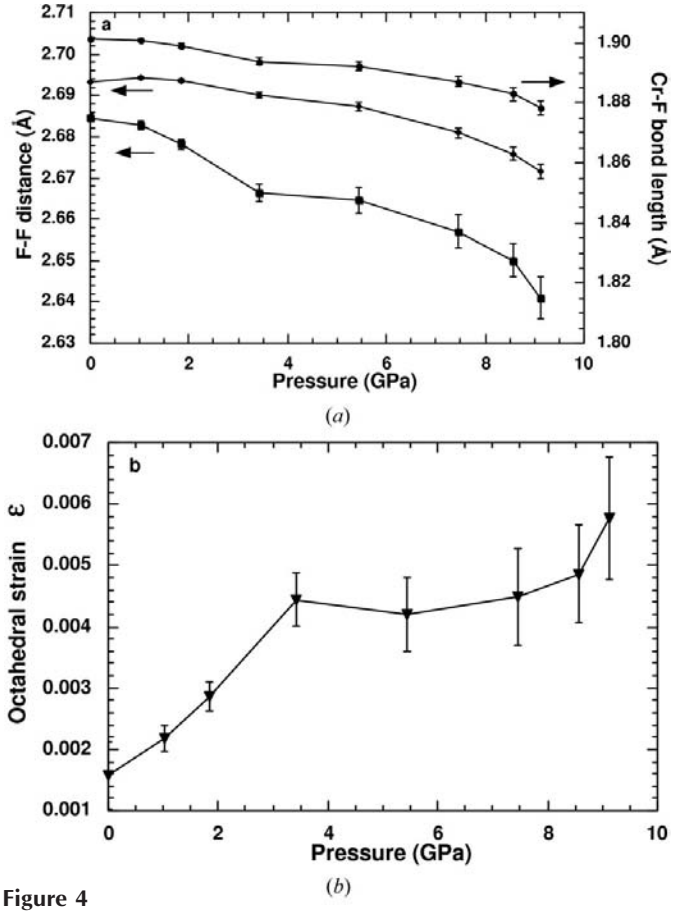

Figure 4
(*a*) The Cr—F bond length (●), F—F distances (d_1: ■; d_2: ◆) and (*b*) octahedral strain ε (▼) plotted as a function of pressure. The octahedral strain is seen to increase linearly up to 3.4 GPa and remains almost constant above this pressure. The increased octahedral strain reflects an elongation of the octahedra along the *c* axis. Solid lines are guides to the eye.

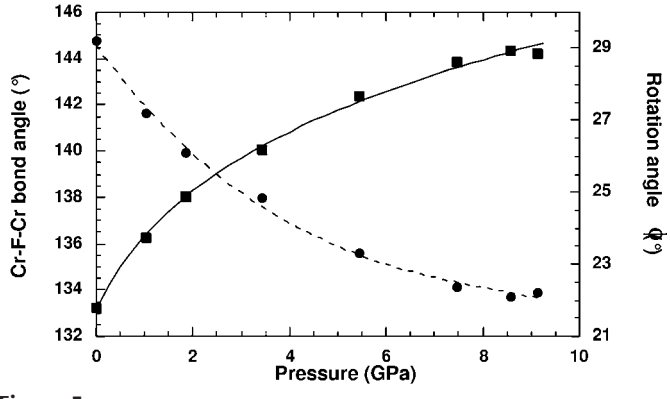

Figure 5
Cr—F—Cr angle (●) and rotation angle φ (■) of the octahedra plotted as a function of pressure. A structure with hexagonally packed fluoride ions corresponds to a Cr—F—Cr angle of 132°. The dotted line is a guide to the eye, while the solid line represents a fit to a power law, as described in the text.

modulus at *ca* 8 GPa, as was the case at 38 GPa for the $R\bar{3}c$ phase of ReO_3 (Jørgensen *et al.*, 2000).

The pressure dependence of φ is shown in Fig. 5 and it is seen that φ obeys the power law $\varphi \propto (P - P_c)^{\beta}$ with β = 0.121 (9) and P_c = −0.9 (2) GPa over the entire range of measured pressures. A similar analysis of the data for FeF_3 and TiF_3 reported by Sowa & Ahsbahs (1998) yielded β = 0.19 (1) for both compounds. Several perovskite compounds undergo temperature or pressure-induced structural phase transitions in which the rotation angle of the octahedra is the order parameter. The pressure or temperature dependence of the low-symmetry phase of these compounds resembles the compression of CrF_3 as the $R\bar{3}c$ structure of this compound can be derived from a hypothetical cubic $Pm\bar{3}m$ phase by rotation of the CrF_6 octahedra around one of the cubic body diagonals. The rotation angle φ is then playing the role of the order parameter. The exponents obtained for CrF_3, FeF_3 and TiF_3 are surprisingly low in comparison with the exponents obtained for other perovskite compounds undergoing structural phase transitions in which the rotation angle of the octahedra is the order parameter. Na_xWO_3 is one example of a perovskite compound undergoing a temperature-induced structural phase transition for which the rotation angle φ was found to obey the power law $\varphi \propto (T_c - T)^{1/2}$ over the entire measured temperature range (Sato *et al.*, 1982). The exponent of 1/2 indicates that Na_xWO_3 obeys mean-field theory. Later it was shown that the rotation angle φ of the ReO_6 octahedra in the $Im\bar{3}$ phase of ReO_3 obeys a power law with the exponent β = 0.322 (5) and critical pressure P_c = 0.5 GPa (Jørgensen *et al.*, 1986). The power law was obeyed over the pressure range from 0.5 to 2.74 GPa, indicating either an unusually large critical region or the proximity of a tricritical point. Furthermore, tricitical behaviour has been observed in uniaxially stressed $RbCaF_3$. The temperature dependence of the rotational order parameter was found to follow a power law, as in the case of Na_xWO_3, but with β = 0.18 (2) (Buzaré *et al.*, 1979). A comparison of the pressure dependence of the rotation angle of the octahedra in CrF_3 and the above-mentioned perovskites is complicated by the fact that CrF_3 is not undergoing a pressure-induced structural phase transition as $\varphi \simeq 22^{\circ}$ at ambient pressure in this compound. However, NbO_2F provides an example of a compound undergoing a pressure-induced phase transition from the cubic ReO_3-type structure ($Pm\bar{3}m$) to the rhombohedral VF_3-type structure ($R\bar{3}c$). The O and F atoms in NbO_2F are statistically distributed over the oxygen sites of the ReO_3 structure and the $Pm\bar{3}m$ to $R\bar{3}c$ transition takes place at 0.47 GPa (Carlson *et al.*, 2000). The compression mechanism of the high-pressure phase is very similar to that observed for TiF_3, FeF_3 and CrF_3. The rotation angle of the $Nb(O,F)_6$ octahedra was found to obey the above-described power law with β = 0.21 (1) or 0.14 (1), depending on the method of calculation, indicating a first-order or tricritical phase transition. The larger value was obtained when φ was calculated from the refined lattice parameters, while calculations based upon the refined x coordinates for the mixed oxygen–fluorine site yielded the lower value. The β values obtained for NbO_2F are in good agreement with the values obtained for FeF_3, TiF_3 and CrF_3, although these compounds do not undergo a $Pm\bar{3}m$ to $R\bar{3}c$ phase transition at a finite pressure.

4. Conclusion

The present study shows that compression of CrF_3 takes place through rotation of the CrF_6 octahedra around the c-axis direction, with only minor changes being observed for the Cr—F bond lengths and the F—F distances within the octahedra (1.2 and 1.6% at 9 GPa, respectively). A small octahedral strain was found to develop during compression, reflecting an elongation of the CrF_6 octahedra along the c-axis direction. No structural phase transitions were observed within the investigated pressure range. The F atoms were found to become hexagonally close packed at *ca* 8 GPa. Furthermore, CrF_3 was found to be relatively soft with a bulk modulus B_o = 29.2 (4) GPa. The rotation angle φ of the octahedra was found to obey the relation $\varphi \propto (P - P_c)^{\beta}$ with β = 0.121 (9).

This work was supported by the EU Framework Programme 5 'Access to ISIS Neutrons'. Mr D. J. Francis is acknowledged for providing technical assistance during the operation of the Paris–Edinburgh pressure cell.

References

Besson, J. M., Nelmes, R. J., Hamel, G., Loveday, J. S., Weill, G. & Hull, S. (1992). *Physica B*, **180–181**, 907–910.
Buzaré, J. Y., Fayet, J. C., Berlinger, W. & Müller, K. A. (1979). *Phys. Rev. Lett.* **42**, 465–468.
Carlson, S., Larsson, A.-K. & Rohrer, F. E. (2000). *Acta Cryst.* B**56**, 189–196.
Decker, D. L. (1971). *J. Appl. Phys.* **42**, 3239–3244.
Fischer, W. (1973). *Z. Kristallogr.* **138**, 129–146.
Grosse, L. & Hoppe, R. (1987). *Z. Anorg. Allg. Chem.* **552**, 123–131.
Hepworth, M. A., Jack, K. H., Peacock, R. D. & Westland, G. J. (1957). *Acta Cryst.* **10**, 63–69.
Herzig, P. & Zemann, J. (1993). *Z. Kristallogr.* **205**, 85–97.
Jack, K. H. & Maitland, R. (1957). *Proc. of the Chem. Soc. (London)*, pp. 232–232.
Jørgensen, J.-E., Jorgensen, J. D., Batlogg, B., Remeika, J. P. & Axe, J. D. (1986). *Phys. Rev. B*, **33**, 4793–4798.
Jørgensen, J.-E., Olsen, J. S. & Gerward, L. (2000). *J. Appl. Cryst.* **33**, 279–284.
Knox, K. (1960). *Acta Cryst.* **13**, 507–508.
Larson, A. C. & Von Dreele, R. B. (1987). Report No. LA-UR-86-748. Los Alamos National Laboratory, New Mexico, USA.
Lösch, R. von, Hebecher, ch. & Ranft, Z. (1982). *Z. Anorg. Allg. Chem.* **491**, 199–202.
Marshall, W. G. & Francis, D. J. (2002). *J. Appl. Cryst.* **35**, 122–125.
Meisel, K. (1932). *Z. Anorg Allg. Chem.* **207**, 121–128.
Sato, M., Grier, B. H., Shirane, G. & Akahane, T. (1982). *Phys. Rev. B*, **25**, 6876–6885.
Sowa, H. (1997). *Acta Cryst.* B**53**, 25–31.
Sowa, H. & Ahsbahs, H. (1998). *Acta Cryst.* B**54**, 578–584.